Tropical SST Response to Global Warming in the Twentieth Century

XIAOJIE ZHU AND ZHENGYU LIU

Center for Climatic Research, University of Wisconsin—Madison, Madison, Wisconsin, and Physical Oceanography Laboratory, Ocean University of China, Qingdao, Shandong, China

(Manuscript received 25 July 2007, in final form 4 August 2008)

ABSTRACT

The trend of sea surface temperature (SST) in the twentieth century is examined in observations and the Intergovernmental Panel on Climate Change (IPCC) twentieth-century simulations. The observed SST neither shows a clear signal of the enhanced equatorial response (EER) warming nor exhibits a clear trend of the El Niño–like warming in the last century. Similarly, the IPCC simulations show neither a clear EER warming nor an El Niño–like warming in the last century. Furthermore, the comparison of heat fluxes in model simulations of the global warming scenario and the twentieth century indicates that the aerosol cooling effect, opposite to the greenhouse gases warming effect, plays an important role in the twentieth century and explains the EER-like signal in the twentieth-century simulations. Therefore, a conclusion that the IPCC model simulations of the twentieth century are consistent with observations within the error bars as well as the future projection of the EER warming pattern in the global warming scenario are validated.

1. Introduction

The response of tropical sea surface temperature (SST) to global warming is important because tropical SST is a major driving force of global climate. Previous studies have focused on the response of the zonal SST gradient along the equator, but with conflicting results. Some favor a La Niña–like response (warming more in the west than in the east; Cane et al. 1997), while others prefer an El Niño–like response (warming more in the east than in the west; Knutson and Manabe 1998; Liu 1998; Yu and Boer 2002; Koutavas et al. 2002; Adams et al. 2003). These controversies led to the question of whether there is a robust signature of tropical SST response to the global warming. Liu et al. (2005, Liu05 hereafter) shed new light on the SST response by focusing on the meridional SST gradient between the equator and the subtropics. Based on the analyses of the transient 1% CO_2 experiments from 14 fully coupled ocean–atmosphere GCMs in the Intergovernmental Panel on Climate Change (IPCC) Fourth Assessment Report (AR4), Liu05 proposed a robust SST response pattern to global warming known as the enhanced equatorial response (EER), which is much more robust than the El Niño–like response. Their results can be summarized in Fig. 1, but now with 17 models [16 IPCC AR4 models and the Fast Ocean Atmosphere Model (FOAM)] in their 1% CO_2 experiments. The meridional gradient of Pacific SST shows a clear EER warming pattern across the models (figure not shown) and in the multimodel ensemble mean (Fig. 1a).[1] There are a maximum warming center in the eastern tropical Pacific and two relative weaker warming centers of the eastern boundary in the extratropical region. After doing the zonal mean of SST over tropical Pacific, a robust EER structure appears on the normalized zonal mean SST trend (Fig. 1b). Here, the SST trend has been normalized by the model sensitivity that is the Pacific mean SST trend, similar as that in Liu05. In comparison to the consistency of EER features across models, the responses in the zonal SST gradient along the equator have a wide spread among models. It shows no clear preference toward an El Niño–like or a La Niña–like response, although the final ensemble mean SST trend shows a slight El Niño–like response with the maximum warming in the eastern Pacific (Fig. 1c). This diverse

Corresponding author address: Xiaojie Zhu, Department of Atmospheric Science, 3150 TAMU, Texas A&M University, College Station, TX 77843.
E-mail: xiaojieer@tamu.edu

[1] The multimodel ensemble mean is the average of all models' normalized SST trends, with each model's SST trend normalized by its Pacific (30°S–30°N, 120°E–80°W) mean SST trend.

DOI: 10.1175/2008JCLI2164.1

© 2009 American Meteorological Society

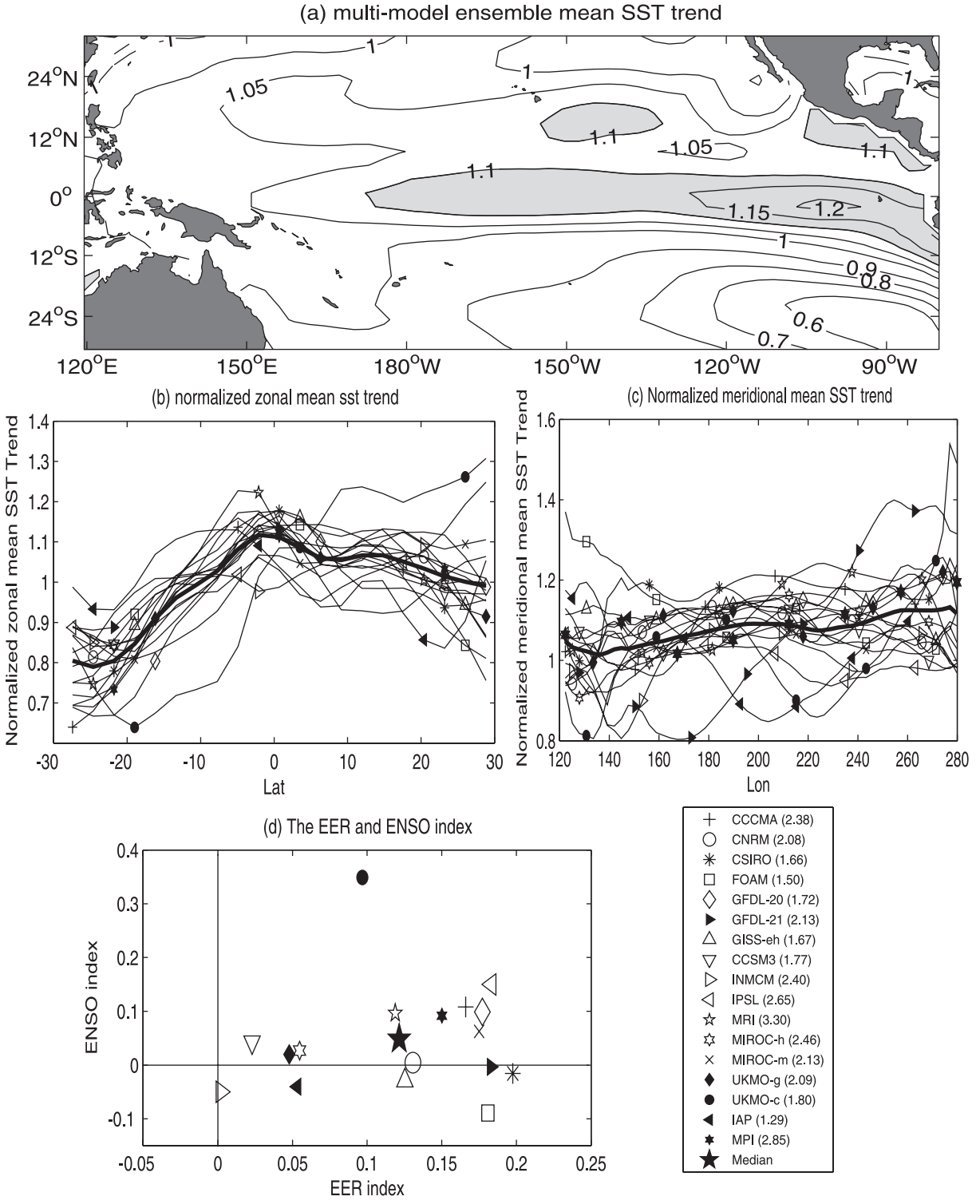

FIG. 1. (a) The multimodel ensemble mean SST trend, (b) the normalized zonal mean SST trends, (c) the normalized meridional mean SST trends, and (d) the EER index vs the ENSO index in the transient 1% CO_2 experiment. The numbers in the label are the climate sensitivities of each model.

response of zonal SST gradient along the equator is consistent with a previous analysis of an independent set of climate model simulations [the Coupled Model Intercomparison Project (CMIP2); Collins et al. 2005].

The SST trend can be quantified with two indices, one for the EER response

$$I_{\mathrm{EER}} = T_{\mathrm{EQ}} - 0.5(T_N + T_S),$$

and the other for the El Niño–like response

$$I_{\mathrm{ENSO}} = T_E - T_W.$$

Here, T_{EQ} is the SST trend averaged over the equatorial Pacific (10°S–10°N, 120°E–80°W); T_N and T_S are the SST trends averaged over the northern (10°–30°N, 120°E–80°W) and southern (10°–30°S, 120°E–80°W) subtropical Pacific, respectively; and T_W and T_E are the SST trends averaged over the western (10°S–10°N, 140°E–160°W) and eastern (10°S–10°N, 160°–100°W) Pacific, respectively. To make the indices comparable across models, each index in each model is divided by its own climate sensitivity. A positive I_{EER} and a positive I_{ENSO} thus represent an EER warming and an El Niño–like warming, respectively. As shown in Fig. 1d, all of the 17 models exhibit $I_{\mathrm{EER}} > 0$, while 11 models show $I_{\mathrm{ENSO}} > 0$, and the remaining 6 models show the opposite ($I_{\mathrm{ENSO}} < 0$). The median of the 17 models' indices shows a positive EER and ENSO index. But the magnitude of the EER warming is about 5 times of that of the El Niño–like warming. Furthermore, the standard deviation for EER indices $\sigma(I_{\mathrm{EER}})^2 = 3.8 \times 10^{-3}$ is smaller than that for ENSO indices $\sigma(I_{\mathrm{ENSO}})^2 = 1.0 \times 10^{-2}$, indicating a much larger diversity in the El Niño–like response than the EER warming.

Such robust EER feature is detected from the global warming scenario simulated in the IPCC models. This brings up a key question: whether this EER feature in the transient 1% CO_2 experiments is a model bias. One way to answer this question is to compare the same models' simulation of the twentieth century with the observation. If the observation does not show a clear EER signal, while the model simulations of the twentieth century still show robust EER signal, then the above mentioned robust EER feature in the global warming scenario would most likely be caused by the model bias. On the other hand, if the simulation of the twentieth century is consistent with the observation within the error bars, a conclusion that models do not bias toward the EER warming pattern can be drawn. In what follows, we examined the Pacific SST trend in the twentieth century both in the observation and the IPCC models' twentieth-century simulations along this line of reasoning.

2. SST trends in the observation

Part of the previous inconsistency of historical SST trend in the observation may be caused by using different datasets and different time periods. For example, Cane et al. (1997) used the Kaplan SST for the period from 1900 to 1991, showing a La Niña–like warming, while Knutson and Manabe (1998) used the Global Sea Ice and Sea Surface Temperature dataset (GISST2) from 1949 to 1994, presenting an El Niño–like warming. We used two observation datasets: the Hadley Center Sea Ice and Sea Surface Temperature from 1870 to 2002 (HadISST; Rayner et al. 2003) and the Extended Reconstructed Sea Surface Temperature from 1900 to 1999 (ERSST; Smith and Reynolds 2003; the result from the Kaplan SST is not shown, for it is similar to the HadISST) and examined two periods: one starts from 1900 and the other from 1950.

The SST trends in observations on the tropical region since 1900 are much more uncertain than those since 1950. Since 1900, the zonal gradients in the two datasets show opposite response patterns: a La Niña–like warming in the HadISST as in Cane et al. (1997), with a small warming trend in the west and a cooling trend in the central and eastern Pacific (Fig. 2a), but an El Niño–like warming in the ERSST, with a basinwide tropical warming centered in the eastern Pacific (Fig. 2c). Since 1950, however, both datasets show a strong El Niño–like warming with the warming maximum center located in the eastern Pacific and a cooling in the North Pacific, the latter likely being the result of the aerosol effect (Figs. 2b,d). The meridional mean SST trends hence support the discussion above (figure not shown). Quantitatively, the ENSO indices (I_{ENSO}) in the two observation datasets are of opposite signs since 1900 (Fig. 3b), but of the same sign since 1950 with discrepancy on the magnitudes (Fig. 3d). Therefore, neither the El Niño–like warming nor the La Niña–like warming can be diagnosed in the above observations, although both observations show an El Niño–like warming in the last 50 yr.

The observed meridional SST gradient in the Pacific between the tropical region and the subtropical region shows similar uncertainty. Since 1900, the SST exhibits an EER warming in the ERSST, with a warming stronger along the equator than that in the subtropics (Fig. 2c). But it exhibits an anti-EER response in the HadISST, with a cooling in the equatorial region and a warming in the subtropics (Figs. 2a). Since 1950, the SST trends are consistent with EER warming in both datasets (Figs. 2b,d). The larger uncertainty of meridional SST gradient change since 1900 than that since 1950 can be observed clearly in the normalized zonal mean SST trend in the Pacific and the indices (Fig. 3). The

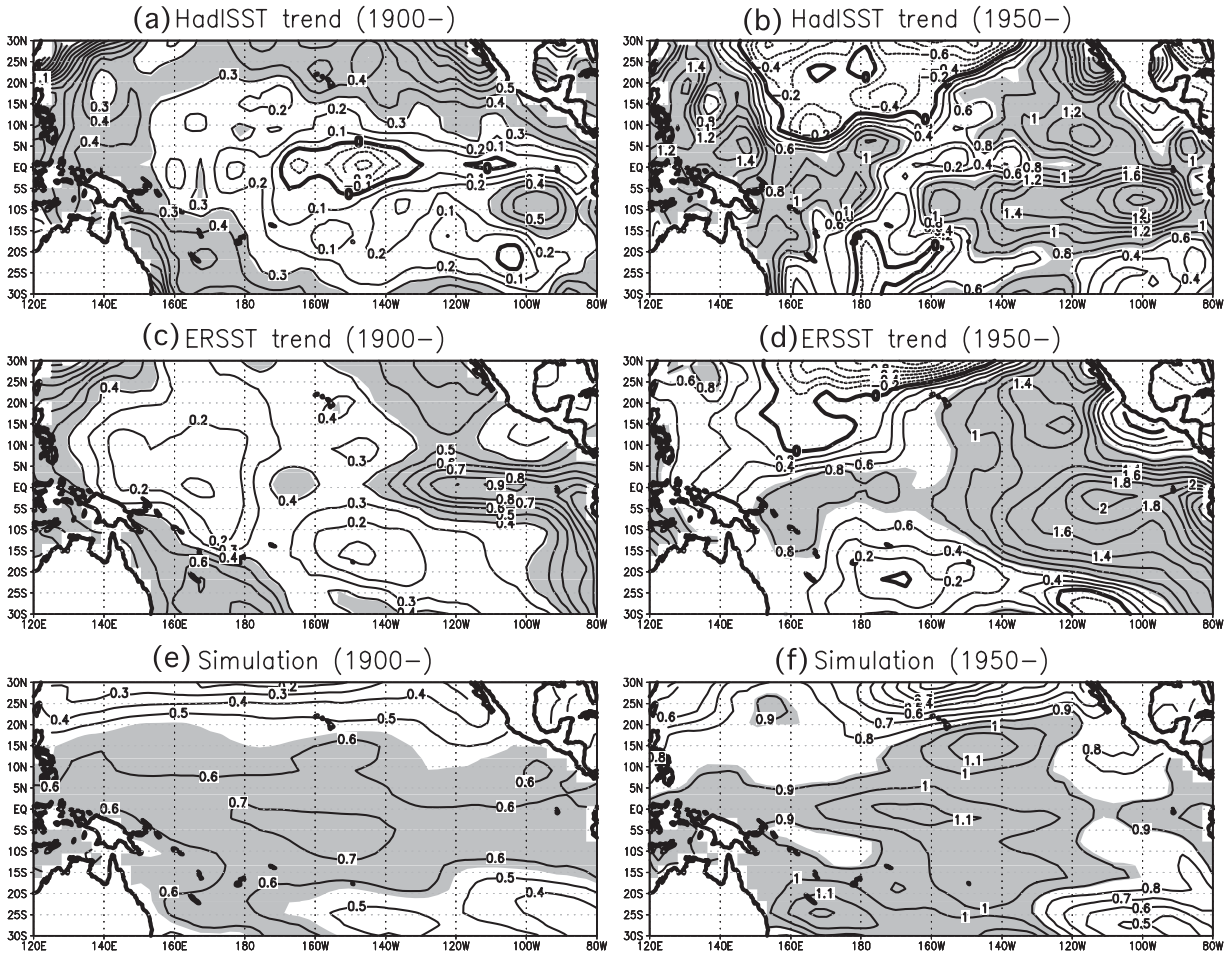

FIG. 2. The observed SST trend in the HadISST (a) since 1900 and (b) since 1950, in the ERSST (c) since 1900 and (d) since 1950, and the multimodel ensemble mean of SST trend in the 15 model simulations (e) since 1900 and (f) since 1950. Shaded for the value above the Pacific mean.

normalized zonal mean SST trends since 1900 in observations are almost out of phase in tropical region (Fig. 3a), and the indices since 1900 show positive EER index in the ERSST and negative EER index in the HadISST (Fig. 3b). After 1950, the two observations tend to show similar EER features in the normalized zonal mean SST trends (Fig. 3c) and nearly the same EER indices (Fig. 3d).

However, the uncertainty in the historical SST shows a fundamental difficulty in the detection of either EER or El Niño–like responses in the observations. The shorter-term trend since 1950 is more consistent, with both datasets showing EER feature, though it is likely to be contaminated by the multidecadal Pacific climate variability or aerosol effect (Minobe 1997; Reader and Boer 1998; Deser et al. 2004). The longer-term trend since 1900 is less likely to be distorted by Pacific decadal variability, but suffers from the poor quality of data in the early period. Therefore, neither a clear EER nor an El Niño–like response can be detected in the observation with high confidence.

3. SST trends in models

The historical SST trend, although with a large uncertainty, can still be used as criteria to judge the models' ability to simulate anthropogenic influence. In the transient 1% CO_2 experiments, a robust EER warming response rather than an El Niño–like warming response appears in the model simulations. If the same models' simulations of the twentieth century show a clear EER response widely beyond the uncertainty of the observation, then the models can be considered strongly biased toward the EER warming response. Otherwise, the robust EER phenomenon in the global warming scenario is not proven artificial.

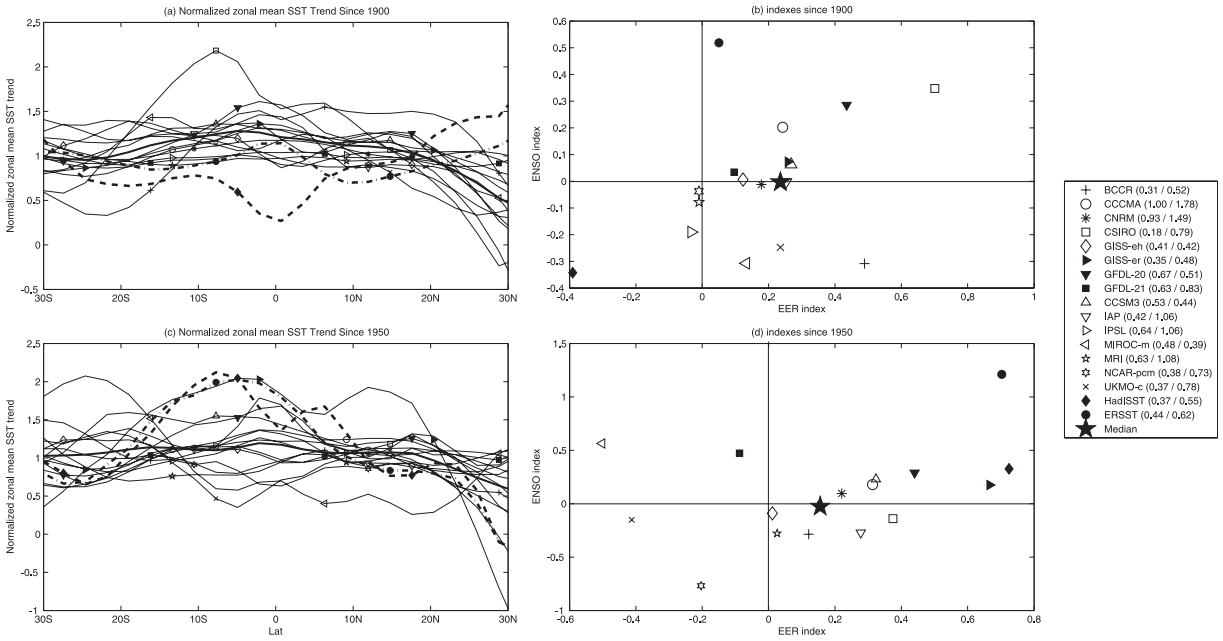

FIG. 3. Normalized Pacific zonal mean SST trends (a) since 1900 and (c) since 1950 and the EER index vs the ENSO index (b) since 1900 and (d) since 1950 in the observations and the IPCC twentieth-century simulations. The numbers in label are the climate sensitivity of each model during the two periods, respectively.

We examined 15 models from the IPCC AR4 assessment of their twentieth-century simulations. The models are the Bjerknes Centre for Climate Research (BCCR) from Norway, the Canadian Centre for Climate Modelling and Analysis (CCCMA) from Canada, the Centre National de Recherches Météorologiques (CNRM) from France, the Commonwealth Scientific and Industrial Research Organisation (CSIRO) from Australia, the Goddard Institute for Space Studies (GISS; model E-H and model E-R) from the National Aeronautics and Space Administration (NASA), the Geophysical Fluid Dynamics Laboratory (GFDL; cm2.0 and cm2.1) from the National Oceanic and Atmospheric Administration (NOAA), the Institute of Atmospheric Physics (IAP) from China, L'Institut Pierre-Simon Laplace (IPSL) from France, the Model for Interdisciplinary Research on Climate (MIROC) and Meteorological Research Institute (MRI) from Japan, the Parallel Climate Model (PCM1) and Community Climate System Model, version 3 (CCSM3) from the National Center for Atmospheric Research (NCAR) and the Met Office (UKMO) Hadley Centre Coupled Ocean–Atmosphere General Circulation Model (HadCM). To compare with the observation, all the model simulations were analyzed in the same periods as those used in the observation analysis.

In the multimodel ensemble mean, at first sight, tropical SST trend appears to be consistent with an EER warming for both time periods with a warming center on the equatorial central Pacific (Figs. 2e,f). The median model SST response is similar to the multimodel ensemble mean (figure not shown). The normalized zonal mean SST trend since 1900 is not as robust as the one under the global warming scenario, but it still shows a weak EER feature (Fig. 3a). However, there are also another two warming centers located in the subtropical region after 1950 except the warming center on the central tropical Pacific (Fig. 2f). Therefore, the normalized zonal mean SST trend since 1950 is almost flat with EER-like feature between the tropical Pacific and the subtropical Pacific (Fig. 3c). The indices in both time ranges show that the majority of the models appear to be consistent with an EER warming but vary in a wide range. Hence, the medians of the indices indicate that the average model simulation shows an EER warming and stands neutral between the El Niño– and La Niña–like warming (Figs. 3b,c). Furthermore, the standard deviations of the EER indices are $\sigma(I_{\mathrm{EER}})^2 = 0.04$ since 1900 and $\sigma(I_{\mathrm{EER}})^2 = 0.10$ since 1950, which are much larger than those in the transient 1% CO_2 experiments, indicating larger diversity of simulated meridional SST gradient changes among the models.

One may conclude that the models show an EER warming response in the twentieth century, which is not consistent with the observation, and therefore the models bias toward the EER warming. However, one

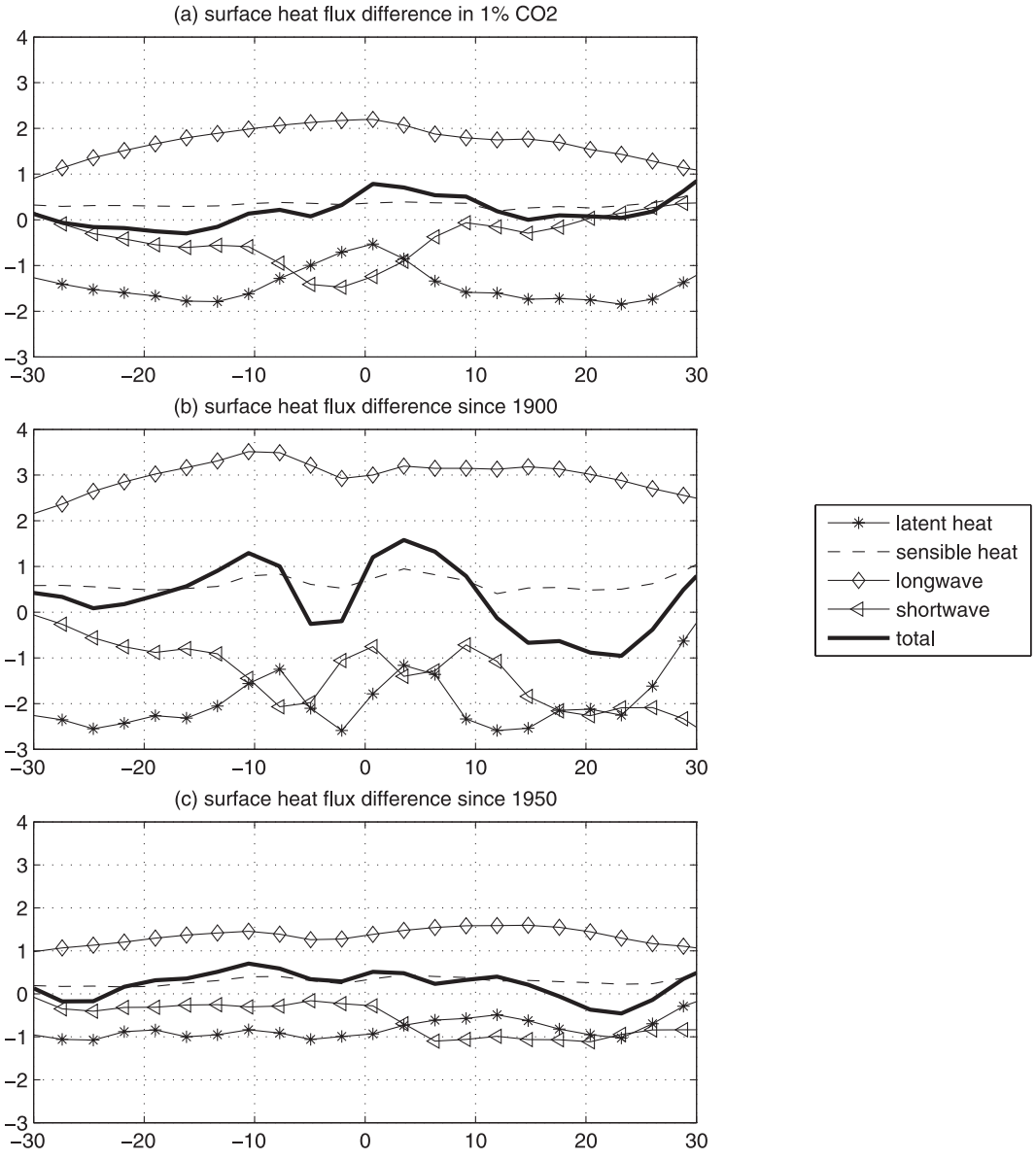

FIG. 4. Zonal mean multimodel ensemble mean differences of the surface heat fluxes between the last 20 yr and the first 20 yr of (a) the transient 1% CO_2 experiments, (b) the twentieth-century simulations since 1900, and (c) the twentieth-century simulations since 1950.

should be cautious in drawing this conclusion. The EER warming detected in the transient CO_2 experiments is determined more by the response in the southern subtropics under the forcing of increased greenhouse gas (Fig. 1b), while the EER signal in the twentieth-century simulations is mostly dominated by the response in the Northern Hemisphere, where there is a large anthropogenic aerosol cooling effect (Figs. 3a,c). As we know, CO_2 and aerosol have different radiative forcing on climate: the former traps the longwave radiation and warms the climate, while the latter blocks the shortwave radiation and cools the planet (Reader and Boer 1998). In warmer climates, the greenhouse gases will trap the longwave radiation and cause the increased net surface downward longwave radiation (Fig. 4). But after 1950, industrial development and volcanic activity have introduced more aerosols in the Northern Hemisphere than in the Southern Hemisphere. Therefore, the net surface shortwave radiation in the twentieth century is asymmetric in two hemispheres, with the Northern Hemisphere gaining less shortwave radiation (Figs. 4b,c). The above analysis indicates that that the aerosol

cooling effect, opposite to the greenhouse warming effect, plays an important role in the twentieth century. This leads to the seemingly significant increase of meridional SST gradient in the Northern Hemisphere. Therefore, in the twentieth-century simulations, the CO_2-induced meridional SST gradient change, if any, is likely small in the Southern Hemisphere.

Compared with the robust greenhouse gases–induced EER feature in transient 1% CO_2 experiments, the EER signal in the twentieth-century simulations is not very robust. Using the FOAM model, Liu05 detected the mechanism of the EER and found it more related to latent heat flux, surface shortwave radiation, and surface ocean mixing. Hence, to better understand the EER-like response in the twentieth century, we analyzed the surface heat flux (Fig. 4). In transient 1% CO_2 experiments from IPCC, there is less latent heat loss from the ocean and more longwave radiation gained by the ocean in the tropical region than that in the subtropical region. The extra heat gained by the tropical ocean favors the EER feature. The contribution of sensible heat flux to the EER response is very small, while the shortwave radiation even favors an anti-EER pattern (Fig. 4a). But the magnitude of shortwave radiation change in subtropical region is much smaller than that of longwave radiation. Therefore, the total heat flux still favors the EER pattern (Fig. 4a). Consequently, there is an extra net surface heat flux gained by the tropical ocean, which may contribute to the EER warming response in the global warming scenario.

However, in the twentieth-century simulations, the changes of turbulent heat fluxes in tropical region and the southern subtropical region are almost equal. And the discrepancies of the changes in surface net radiation flux between the tropics and the southern subtropics are also small. Hence, there is small difference of the anomalous net surface heat flux into the ocean between the tropics and the southern subtropics. This favors no EER pattern between the tropics and the Southern Hemisphere (Figs. 4b,c). The changes of latent heat flux, sensible heat flux, and longwave radiation in the Northern Hemisphere are similar to that in the Southern Hemisphere. But the change in shortwave radiation demonstrates a stronger decrease in the Northern Hemisphere (Figs. 4b,c), especially after 1950 (Fig. 4c), which may be a result of the increased aerosol in the twentieth century. With the large decrease of shortwave radiation in the Northern Hemisphere, the net surface heat flux in Northern Hemisphere is decreased and contributed to this EER-like pattern in the twentieth century, which is not mainly caused by the increasing greenhouse gas. Therefore, in the twentieth century, the greenhouse gases–induced EER warming is not clear.

It is also interesting to observe that the equatorial SST warming centers in the model simulation occur not in the eastern and western Pacific, but in the central Pacific (about 170°W) in both periods (Figs. 2e,f), which differ significantly from both observations. Furthermore, the equatorial SST response shows a wide spread in the twentieth-century simulations between the El Niño– and La Niña–like responses (Figs. 3b,d), similar to that in the transient CO_2 simulations (Figs. 1c,d; Collins et al. 2005), with the standard deviations of the ENSO indices being $\sigma(I_{\mathrm{ENSO}})^2 = 3.9 \times 10^{-2}$ since 1900 and $\sigma(I_{\mathrm{ENSO}})^2 = 0.12$ since 1950 (Figs. 3b,d). Hence, the model's prediction of the zonal SST gradient change still keeps its large uncertainty.

4. Summary

In the twentieth century, neither the EER nor the El Niño–like responses can be identified clearly in both observations and model simulations. There are two possible reasons for the difference between observations and model simulations: the first is the quality of the observation datasets and the other is the different causes of the twentieth-century warming pattern. In the simulations of the twentieth-century climate, some models did not include the effect of volcanic eruptions in their experiment design. This can explain the warmer climate in the twentieth-century simulations than that in the observations. Furthermore, besides the greenhouse gas warming effect, there are also another important aerosol cooling effect influenced the twentieth century's climate, especially after 1950. Hence, a strong cooling response in the Northern Hemisphere is shown in both observations and model simulations, which contributes to an EER-like pattern. Therefore, considering the similarity between observations and model simulations (that none of them shows a clear greenhouse gases–induced EER warming signal), the simulated meridional SST gradients of the twentieth century in IPCC models are acceptable within all these error bars.

In the transient 1% CO_2 forcing experiments, the Southern Hemisphere warms less than the Northern Hemisphere (Fig. 1b), whereas in the twentieth-century simulations the Southern Hemisphere warms more than the Northern Hemisphere (Figs. 3a,c). As a result, the warming response in the southern subtropics makes a greater contribution to the EER warming pattern under the forcing of the increased greenhouse gases, while in the twentieth-century simulations many of the models and the observations demonstrate less warming or cooling in the North Pacific, especially after 1950 with rapid industrial developments. Such cooling might be influenced by aerosol pollution, which has stronger

amplitude in the North Pacific than in the South Pacific. For different simulation scenarios, the models demonstrate different physical response. In the global warming scenario, the surface net heat flux increases in the tropical region but decreases in the subtropics. And in a result, it contributes to the EER warming pattern. While in twentieth century the surface net heat flux does not have a large discrepancy between the tropics and the southern subtropics. Therefore, no clear EER patterns can be detected in the Southern Hemisphere. But with a strong decrease of shortwave radiation in Northern Hemisphere, the decreased warming or cooling of the Northern Hemisphere contributes to an EER-like feature in the Northern Hemisphere, which is not mainly caused by the increasing greenhouse gases. Therefore, considering the different dominant forcing factors in the two scenarios in the IPCC models, the models simulated reasonable meridional SST gradient response to different external forcing and do not bias toward the robust EER warming pattern.

For the zonal SST gradient in the twentieth century, both the observations and the IPCC model simulations show similar uncertainty between the El Niño– and the La Niña–like warming. Also, under the global warming scenario with increasing CO_2 concentration, the zonal SST gradient change still remains largely uncertain among models. Therefore, the prediction of future zonal SST gradient in the model is still under progress.

Acknowledgments. The authors thank Dr. Qinyu Liu for helpful discussions. We also acknowledge the international modeling groups for providing the dada. This work is supported by NOAA, DOE, Ocean University of China and the National Natural Science Foundation of China (number 40676010).

REFERENCES

Adams, J. B., M. E. Mann, and C. M. Ammann, 2003: Proxy evidence for an El Niño-like response to volcanic forcing. *Nature,* **426,** 274–278.

Cane, M., A. C. Clement, A. Kaplan, Y. Kushnir, D. Pazdnyakov, R. Seager, S. Zebiak, and R. Murtgudde, 1997: Twentieth-century sea surface temperature trends. *Science,* **275,** 957–960.

Collins, M., and The CMIP Modelling Groups, 2005: El Niño- or La Niña-like climate change? *Climate Dyn.,* **24,** 89–104.

Deser, C., A. S. Phillips, and J. W. Hurrel, 2004: Pacific interdecadal climate variability: Linkages between the tropics and the North Pacific during boreal winter since 1900. *J. Climate,* **17,** 3109–3124.

Knutson, T. R., and S. Manabe, 1998: Model assessment of decadal variability and trends in the tropical Pacific Ocean. *J. Climate,* **11,** 2273–2296.

Koutavas, A., J. Lynch-Stieglitz, T. M. Marchitto Jr., and J. P. Sachs, 2002: El Niño-like pattern in ice age tropical Pacific sea surface temperature. *Science,* **297,** 226–230.

Liu, Z., 1998: On the role of ocean in the transient response of tropical climatology to global warming. *J. Climate,* **11,** 864–875.

——, S. Vavrus, F. He, N. Wen, and Y. Zhong, 2005: Rethinking tropical ocean response to global warming: The enhanced equatorial warming. *J. Climate,* **18,** 4684–4700.

Minobe, S., 1997: A 50–70 year climatic oscillation over the North Pacific and North America. *Geophys. Res. Lett.,* **24,** 683–686.

Rayner, N. A., D. E. Parker, E. B. Horton, C. K. Folland, L. V. Alexander, D. P. Rowell, E. C. Kent, and A. Kaplan, 2003: Global analyses of sea surface temperature, sea ice, and night marine air temperature since the late nineteenth century. *J. Geophys. Res.,* **108,** 4407, doi:10.1029/2002JD002670.

Reader, M. C., and G. J. Boer, 1998: The modification of greenhouse gas warming by the direct effect of sulphate aerosols. *Climate Dyn.,* **14,** 593–607.

Smith, T. M., and R. W. Reynolds, 2003: Extended reconstruction of global sea surface temperatures based on COADS data (1854–1997). *J. Climate,* **16,** 1495–1510.

Yu, B., and G. J. Boer, 2002: The roles of radiation and dynamic processes in the El Niño-like response to global warming. *Climate Dyn.,* **19,** 539–553.